

# Ultrafast Stimulated Emission Microscopy of Single Nanocrystals

Lukasz Piatkowski<sup>1,2\*</sup>, Nicolò Accanto<sup>1#</sup>, Gaëtan Calbris<sup>1‡</sup>, Sotirios Christodoulou<sup>1,3</sup>  
Iwan Moreels<sup>3,4</sup> and Niek F. van Hulst<sup>1,5\*</sup>

<sup>1</sup> ICFO—Institut de Ciències Fotoniques, the Barcelona Institute of Science and Technology, 08860 Castelldefels (Barcelona), Spain.

<sup>2</sup> Institute of Physical Chemistry, Polish Academy of Sciences, Kasprzaka 44/52, 01-224 Warsaw, Poland.

<sup>3</sup> Istituto Italiano di Tecnologia, Via Morego 30, 16163 Genova, Italy.

<sup>4</sup> Department of Chemistry, Ghent University, Krijgslaan 281-S3, 9000 Gent, Belgium.

<sup>5</sup> ICREA—Institut de Recerca i Estudis Avançats, 08010 Barcelona, Spain.

# Present address: Institut de la Vision, Sorbonne Université, Inserm S968, CNRS UMR7210, 17 Rue Moreau, 75012, Paris, France.

‡ These authors contributed equally to this work.

\* E-mail: lukasz.j.piatkowski@put.poznan.pl; Niek.vanHulst@ICFO.eu

## Abstract

Single molecule detection is a powerful method used to distinguish different species and to follow time trajectories within the ensemble average. However, such detection capability requires efficient emitters and is prone to photobleaching, while the slow, nanosecond spontaneous emission process only reports on the lowest excited state. We demonstrate direct detection of stimulated emission from individual colloidal nanocrystals at room temperature, while simultaneously recording the depleted spontaneous emission, enabling us to trace the carrier population through the entire photo-cycle. By capturing the femtosecond evolution of the stimulated emission signal, together with the nanosecond fluorescence, we can disentangle the ultrafast charge trajectories in the excited state and determine the populations that experience stimulated emission, spontaneous emission and excited state absorption processes.

Complex physical, chemical and biological processes are determined by fundamental spatial and temporal interaction trajectories. Only ultrafast techniques with single-emitter sensitivity are able to unveil their inherent transient intermediates and allow exploration of processes such as molecular vibrations and energy transfer (1-3), and nanoscale dynamics in plasmonic or 2D materials (4, 5). The small interaction cross-sections of individual nanoparticles make it difficult to rely on the conventional ultrafast approaches, such as transient absorption and nonlinear four wave mixing. Consequently, single molecules and nanoparticles are almost exclusively detected through Stokes shifted spontaneous emission (fluorescence or photoluminescence (PL)), which is background-free, allowing photon counting sensitivity, and detection of weakly fluorescent emitters. The use of fluorescence detection, however, is hampered by a number of limitations: it is restricted to luminescent samples, is sensitive to bleaching, and in the linear regime it is slow (nanoseconds), reporting only on the population of the final emitting state, while missing out on femtosecond dynamics. Despite the exploration of several alternative detection schemes, such as, photo-thermal (6), linear absorption (7, 8) or enhanced Raman (9), ultrafast detection of single entities beyond fluorescence has remained challenging.

Here we demonstrate a highly sensitive experimental scheme based on the direct detection of stimulated emission (SE) for studying the excited state dynamics in nanoscopic samples with femtosecond temporal resolution. SE microscopy involves one laser pulse for promotion to the excited state, and a second, delayed pulse, for stimulation back to the ground state, generating a new SE photon (10). SE forms the basis of the stimulated emission depletion (STED) microscopy, however, in a typical STED experiment the stimulated photons are discarded and only PL is recorded. Yet, the instantaneous SE photons contain information on the excited state population, its dynamics and relaxation pattern, which is otherwise inaccessible from the slow PL. To its advantage, SE is not critical on the quantum efficiency of the sample, has femtosecond temporal resolution, is coherent, and capable of mapping the dynamics of an arbitrary excited state.

We present direct stimulated emission detection and imaging of individual NCs, and trace the excited state dynamics of single colloidal CdSe/CdS rod-in-rod NCs (11) with femtosecond temporal resolution, at ambient conditions. The PL is detected simultaneously with the SE, generating two independent, complementary images. It is important to understand the dynamic interplay between various charge relaxation pathways, such as charge injection, extraction, transfer and delocalization, and excited state relaxation, both ultrafast and with nanoscopic sensitivity (12-14). Our femtosecond SE experiment on single-NCs, shows the excited state relaxation dynamics of individual charges, the dynamical heterogeneity of NCs and the relative contributions of the various stimulated processes, all with single-NC sensitivity.

A pump beam excites the NC through two-photon absorption to a highly excited state in the conduction band (Fig. 1, details in Materials and Methods (15)). The excited hot electrons and holes, initially localized in the shell, decay through the excited state progression and eventually localize in the lowest excited state (band edge) in the core (Fig. 1C). The probe (stimulation) beam, resonant with the core band-edge transition, leads to charge recombination, stimulates the NC back to the ground state and induces emission of a stimulated photon. Therefore, any information on the excited charges imprinted by the pump beam in the shell is 'read out' by the stimulating probe beam, when one of the excited charges reaches the core band-edge states. The pump beam is modulated, and the SE signal is retrieved by lock-in detection.

In a first step, we raster-scanned the sample while simultaneously detecting both modulated signal ( $S_{\text{mod}}$ ) and PL (Fig. 2A,B). The PL image clearly reveals the NC presence, which we verified through their emission spectra (Fig. S1). The corresponding  $S_{\text{mod}}$  image shows contrast at the same sample positions where the PL signal appears. Moreover, the measured  $S_{\text{mod}}$  signal was always positive, meaning we detected extra photons in our stimulation beam (Supp. Text 1). Two effects can in principle lead to an increase of the transmitted probe beam intensity when the NC is excited: stimulated emission and ground state depletion (GSD). In the first case, the SE process following electron-hole recombination gives a net increase in the probe beam intensity. In the second case, the absorption of the probe beam is lower because of the depletion of the ground state, due to the presence of either hole or electron in their respective energy levels. The two contributions can be readily distinguished by time-resolved experiments, as shown later. For most NCs we found a perfect

correspondance between PL and  $S_{\text{mod}}$  images and observed  $S_{\text{mod}}$  wherever PL appeared (Fig. 2C). Interestingly, in some cases we detected PL, but no measurable  $S_{\text{mod}}$  (Fig. 2E). We assigned this signal to core-free CdS shell nanoparticles that co-nucleated during synthesis. Finally, on rare occasions we observed  $S_{\text{mod}}$  contrast but no PL (Fig. 2D). The signal likely originated from highly quenched NCs, as it is improbable that we observe other particles with the exact same spectral signature. Clearly, the spectral dependence of  $S_{\text{mod}}$  selected with the probe beam, and the ability to detect simultaneously PL and  $S_{\text{mod}}$  gives us extra insight as to the nature of the detected NCs.

Ultrafast coherent response is the main advantage of SE detection. In Figure 3A we show a series PL and  $S_{\text{mod}}$  images for different interpulse-delay (more images in Fig. S2). While PL signal is detected at all time delays  $\Delta t$ , the  $S_{\text{mod}}$  signal appears only when the pump pulse overlaps or precedes the stimulation pulse. At negative delay times, when the stimulation pulse arrives before the pump pulse, the NC is in its ground state and there is no excited state population for the probe pulse to interact with. For the NC marked with  $x$  the second order autocorrelation trace exhibits a dip with  $g^{(2)}(0) \lesssim 0.5$ , indicating the non-classical emission of a single NC (Fig. S3). The time-resolved traces revealed that when  $S_{\text{mod}}$  (blue) increases in time, the PL (red) decreases (Fig. 3B). This is intuitive – the excited state population, which is stimulated down back to the ground state does not contribute to the spontaneous emission, leading to PL depletion. The fact that  $S_{\text{mod}}$  and PL signals are anti-correlated unambiguously indicates that  $S_{\text{mod}}$  contains a significant contribution from the SE process. Furthermore, we found that the changes of both signals:  $S_{\text{mod}}$  ingrowth ( $\Delta S_{\text{mod}}$ ) and PL depletion ( $\Delta \text{PL}$ ), occur on specific timescales. Interestingly, the  $\Delta \text{PL}$  depletion occurs with a single time constant, while  $\Delta S_{\text{mod}}$  grows in with two time constants. The slower time constant of  $\sim 400\text{-}700$  fs is identical to the time with which  $\Delta \text{PL}$  decreases. However, a significant part of the  $S_{\text{mod}}$  grows on a faster timescale, and cannot be observed within the cross-correlation time of the pump and probe pulses ( $<200$  fs). To understand this, one needs to consider that the NCs are initially pumped to a highly excited state in the shell (Supp. Text 3), while the stimulation pulse probes the lowest excited state in the core. GSD occurs when charges are present in the excited state of the transition resonant with the probe energy. As soon as the faster of the two charges reaches the lowest excited state of the core (16-19), the probe beam absorption will decrease. This means that GSD reports on the relaxation rate of the fastest charge, either the electron or the hole. In contrast, the probe beam can induce charge recombination and SE only when both electron and hole localize into the core. Consequently, SE is sensitive to relaxation of the slower of the two charges. In the PL we see only the slower component, because PL is a time averaged signal, which is mostly sensitive to the population decay of the lowest excited state (Supp. Text 4).

We quantified the observed dynamics by simultaneously fitting the PL and  $S_{\text{mod}}$  traces (Supp. Text 5). PL and  $S_{\text{mod}}$  traces acquired on small NC clusters revealed that the average slower charge relaxation time is 550 fs (black histogram in Fig. 3C). The time delay traces recorded repeatedly on the same individual NCs (more traces in Fig. S5) revealed the relaxation heterogeneity among individual NCs (Fig. 3C). From the difference in the dynamics between SE and GSD we determined the relative contribution of the two signals to the total measured signal  $S_{\text{mod}}$ , by performing simple, qualitative kinetic rate equation calculations (Supp. Text 6). The experimental ratio of SE/ $S_{\text{mod}}$  extracted from individual time traces for a large number of NCs centers around a value of  $\sim 0.17$  (Fig. 3D). The observation of a ratio SE/ $S_{\text{mod}} < 0.2$  strongly suggests that the cross-sections for absorption and SE might be somewhat different given the large asymmetry between the shape of the absorption and emission bands.

The lower SE signal with respect to GSD signal might also be caused by an excited state absorption (ESA) process. In ESA, the probe beam promotes the excited charges to higher excited states at the cost of absorbing a probe beam photon, leading to a reduction of the apparent SE contrast, enhanced bleaching (14, 20) and quenching (21). To uncover the role of ESA in our NC dynamics, we varied the duration of the probe pulse, as the ESA timing should be sensitive to the observed 550 fs relaxation time of the hot state. Once the charges have again returned to the emitting state, the probe pulse should stimulate the NC down. The concept, depicted in Fig. 4B, is analogous to STED experiments, where the STED pulse is stretched to prevent re-excitation (22). We measured the  $S_{\text{mod}}$

and  $\Delta\text{PL}$  contrast for increasing probe pulse duration ( $\Gamma$ ), stretched up to 2.5 ps, at  $\Delta t=7$  ps delay. In Fig. 4C both  $S_{\text{mod}}$  and  $\Delta\text{PL}$  show increased contrast with the probe pulse duration. Interestingly, the in-growth matches very well the 550 fs excited state charge relaxation time determined from the pump-probe traces. A simulation using the kinetic rate equation model expanded with the ESA process (Supp. Text 7) reproduces the experimental data well and confirms our hypothesis that stretching the stimulating probe pulse allows to stimulate down charges that otherwise undergo ESA.

Interestingly, the simultaneous detection of stimulated and spontaneous emission of a single NC allows us to correlate the decays in quantitative manner. The number of photons detected in SE should be equal to the number of photons missing in PL, that is PL depletion. For the data shown in Fig. 3B, we determined an effective number of photons depleted from PL,  $\#\Delta\text{PL}_{\text{eff}} = 1.6 \cdot 10^7$  photons/s and an effective number of photons gained in the stimulation beam  $\#\text{SE}_{\text{eff}} = 1.3 \cdot 10^7$  photons/s per NC (Supp. Text 8). The two values are in good agreement, given the fact that the detection occurs in two independent channels, using photon counting vs analogue detectors.

The high sensitivity of the presented SE detection opens up new imaging possibilities of weakly fluorescing or quenched systems, while the time-resolved experiment provides information on the excited state relaxation dynamics and its mechanism, all with femtosecond time resolution and single-emitter sensitivity. The unconventional, simultaneous detection of the spontaneous and stimulated emission provides large imaging specificity: the fact that SE depends on two distinct frequencies, in combination with the inter-pulse time-delay, makes the method extremely sensitive to different species within a dense ensemble.

The time-resolved femtosecond SE experiment allowed to us to provide a comprehensive picture of the excited charges, which are either stimulated down, or promoted to higher excited states, or recombine spontaneously. The SE and GSD contributions comprise  $<20\%$  and  $>80\%$  of the total induced ground/excited state population difference, respectively. This was aided by the fact that the two excited charges, electrons and holes, exhibit different relaxation times (Supp. Text 9). The rod-in-rod CdSe/CdS NCs excited holes localize at the core band edge within 200 fs, while the excited electrons relax to the core band edge on a time scale of 550 fs. We found that the electron relaxation time differs nearly a factor of two between individual NCs. Finally, the single-emitter sensitivity of our experiment allowed us to compare the number of photons lost in PL and gained through SE in absolute terms, which is difficult to achieve for ensembles (23). Stretching the stimulation pulse allowed us to elucidate the presence of ESA and increase the SE efficiency by 40%-50%, i.e. a significant portion of the excited charges undergo ESA and relax back to the core band edge states.

The ultrafast SE microscopy opens up a spectrum of experiments to be explored (Supp. Text 10). Scanning the stimulation pulse energy would allow for state selectivity and enable studying excited state-to-state dynamics (16). Given its coherent nature, SE microscopy could be expanded to accommodate heterodyne detection of the stimulation beam and could provide an easy access to investigating coherent effects such as coherent energy transfer (3, 24). The absorption cross-section of our NCs at the stimulation wavelength is approximately an order of magnitude larger than the absorption cross-section of a typical fluorescent dye ( $3 \cdot 10^{-16}$  cm<sup>2</sup> vs  $10^{-17}$  cm<sup>2</sup>) (25). Therefore, even single molecules could be detected in stimulated emission.

## References and Notes

1. S. Yampolsky *et al.*, *Nat. Photon.* **8**, 650-656 (2014)
2. M. Liebel, C. Toninelli, N. F. van Hulst, *Nat. Photon.* **12**, 45-49 (2018)
3. R. Hildner, D. Brinks, J. B. Nieder, R. J. Cogdell, N. F. van Hulst, *Science* **340**, 1448-1451 (2013)
4. M. Aeschlimann *et al.*, *Science* **333**, 1723-1726 (2011)
5. V. Kravtsov, R. Ulbricht, J. M. Atkin, M. B. Raschke, *Nat. Nanotech.* **11**, 459-464 (2016)
6. A. Gaiduk, M. Yorulmaz, P. V. Ruijgrok, M. Orrit, *Science* **330**, 353-356 (2010)

7. P. Kukura, M. Celebrano, A. Renn, V. Sandoghdar, *J. Phys. Chem. Lett.* **1**, 3323-3327 (2010)
8. S. Chong, W. Min, X. S. Xie, *Phys. Chem. Lett.* **1**, 3316-3322 (2010)
9. A. B. Zrimsek *et al.*, *Chem. Rev.* **117**, 7583-7613 (2017)
10. W. Min *et al.*, *Nature* **461**, 1105-1109 (2009)
11. S. Christodoulou *et al.*, *Nat. Commun.* **6**, 7905-7913 (2015)
12. J. Hanne *et al.*, *Nat. Commun.* **6**, 7127-7133 (2015)
13. M. D. Lesoine *et al.*, *J. Phys. Chem. C* **117**, 3662-3667 (2013)
14. S. E. Irvine, T. Staudt, E. Rittweger, J. Engelhardt, S. W. Hell, *Angew. Chem.* **47**, 2685-2688 (2008)
15. See supplementary material
16. P. Kambhampati, *J. Phys. Chem. C* **115**, 22089-22109 (2011)
17. E. Hendry *et al.*, *Phys. Rev. Lett.* **96**, 057408-057412 (2006)
18. S. Brovelli *et al.*, *Nano Lett.* **14**, 486-494 (2014)
19. M. Zavelani-Rossi, M. G. Lupo, F. Tassone, L. Manna, G. Lanzani, *Nano Lett.* **10**, 3142-3150 (2010)
20. J.-I. Hotta *et al.*, *J. Am. Chem. Soc.* **132**, 5021-5023 (2010)
21. T. Watanabe *et al.*, *Chem. Phys. Lett.* **420**, 410-415 (2006)
22. T. A. Klar, S. W. Hell, *Optics Lett.* **24**, 954-956 (1999)
23. E. Rittweger, B. R. Rankin, V. Westphal, S. W. Hell, *Chem. Phys. Lett.* **442**, 483-487 (2007)
24. A. Chenu, G. D. Scholes, *Annu. Rev. Phys. Chem.* **66**, 69-96 (2015)
25. L. Kastrup, S. W. Hell, *Angew. Chem. Int. Ed.* **43**, 2-5 (2004)
26. N. Accanto *et al.*, *Light Sci. Appl.* **3**, e143 (2014)
27. S. Berciaud, D. Lasne, G. A. Blab, L. Cognet, B. Lounis, *Phys. Rev. B* **73**, 045424 (2006)
28. M. Allione *et al.*, *ACS Nano* **7**, 2443-2452 (2013)
29. D. J. Norris, M. G. Bawendi, *Phys. Rev. B* **53**, 16338-16346 (1996)
30. M. G. Lupo *et al.*, *Nano Lett.* **8**, 4582-4587 (2008)
31. G. Xing *et al.*, *ACS Nano* **6**, 10835-10844 (2012)
32. C. Galland *et al.*, *Nano Lett.* **13**, 321-328 (2013)
33. B. T. Diroll, M. E. Turk, N. Gogotsi, C. B. Murray, J. M. Kikkawa, *Chem. Phys. Chem.* **17**, 759-765 (2016)
34. T. Walz, S. J. Jamieson, C. M. Bowers, P. A. Bullough, C. N. Hunter, *J. Mol. Biol.* **282**, 833-845 (1998)
35. L. Piatkowski, E. Gellings, N. F. van Hulst, *Nat. Commun.* **7**, 10411 (2016)

## Acknowledgements

L.P. acknowledges the Marie Skłodowska-Curie COFUND and the ICFOnest programs. This project has received funding from National Science Centre, Poland, grant 2015/19/P/ST4/03635, POLONEZ 1 and from the European Union's Horizon 2020 research and innovation programme under the Marie Skłodowska-Curie grant agreement No. 665778. This research was funded by the European Commission (ERC Advanced Grant 670949-LightNet), the Spanish Ministry of Economy MINECO (FIS2012-35527, FIS2015-72409-EXP, FIS2015-69258-P, Network FIS2016-81740-REDC 'NanoLight' and Severo Ochoa Grant SEV2015-0522), the Catalan AGAUR (No. 2017SGR1369), Fundació Privada Cellex, Fundació Privada Mir-Puig, and Generalitat de Catalunya through the CERCA Program. **Author contributions:** L.P. and N.F.v.H. designed the experiment. L.P., N.A. and G.C. performed the experiments and data analysis. S.C. and I.M. provided the samples. L.P. and N.F.v.H. wrote the manuscript. All authors discussed the results and commented on the manuscript. **Competing interests:** The authors declare no competing financial interests. **Data and materials availability:** All data are available in the main text or in the supplementary materials (26-35).

**Supplementary Materials**  
 Materials and Methods.  
 Supplementary Text 1 to 10.  
 Supplementary figures S1 to S12.  
 References 26-35

**Figures**

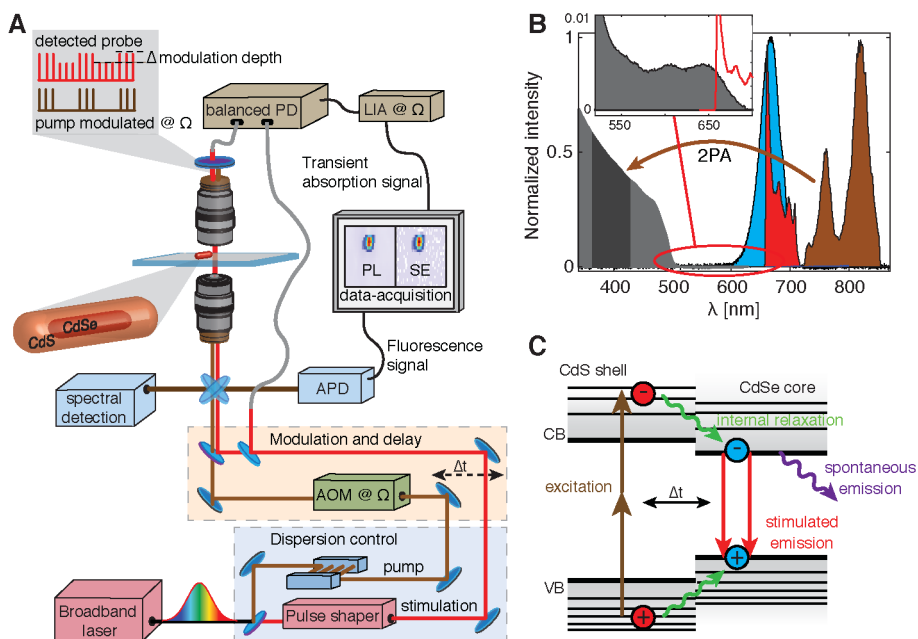


**Fig. 1. Concept of the ultrafast stimulated emission nanoscopy. (A)** Schematic of the experimental setup. **(B)** Spectral characteristics of the broadband laser pulse (pump pulse - brown, probe pulse - red) and CdSe/CdS NCs. Grey and blue shaded areas represent absorption and emission spectrum of the NCs, respectively. The black area indicates the spectral range of the two-photon absorption. **(C)** Energy level sketch of a core/shell CdSe/CdS NC.

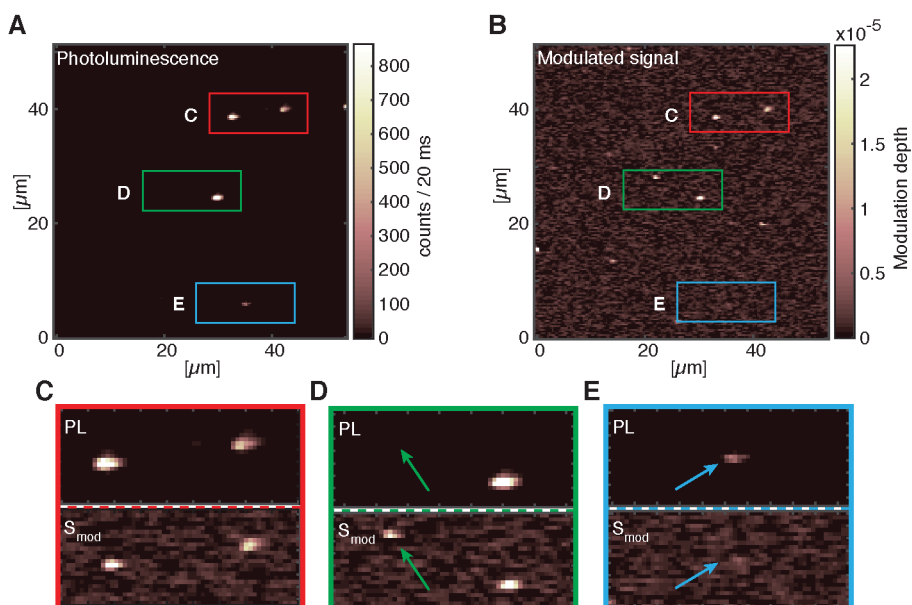


**Fig. 2. Stimulated emission imaging.** (A, B) Confocal images of the same sample area showing PL and lock-in signal ( $S_{\text{mod}}$ ), respectively. The stimulation beam was set to arrive 7 ps after the pump beam (Supp. Text 2). (C-E) Comparison between the PL and  $S_{\text{mod}}$  images for the three regions of interest marked in panels A and B.

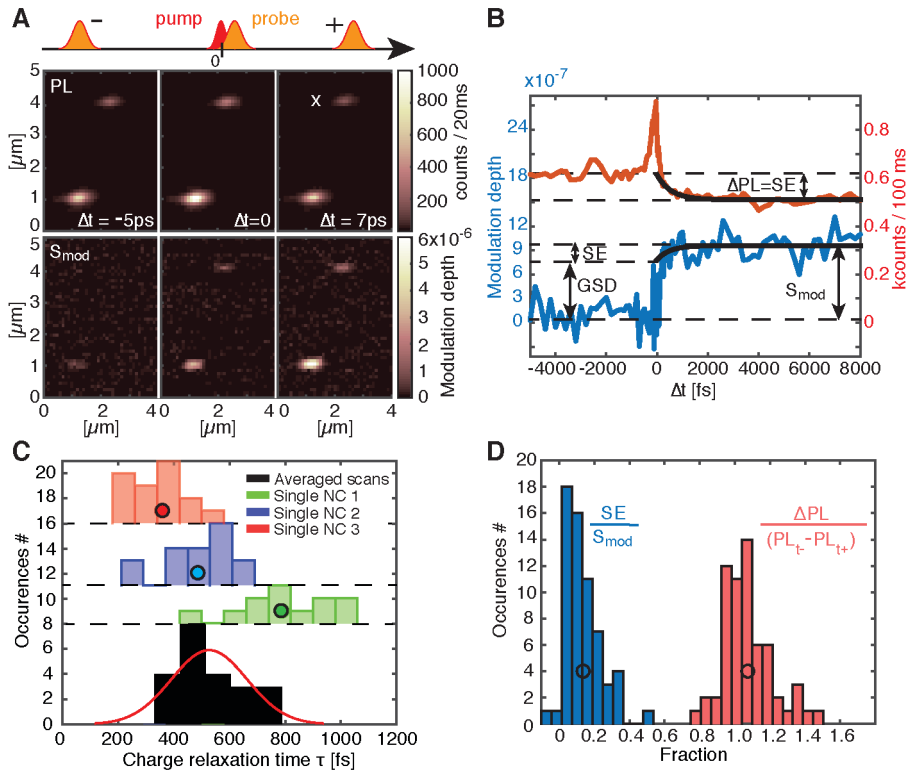


**Fig. 3. Time-resolved stimulated emission microscopy.** (A) A series of images acquired by detecting PL and  $S_{\text{mod}}$  signal, for different excitation and stimulation interpulse delays  $\Delta t$ . (B) Simultaneously detected  $S_{\text{mod}}$  (blue) and PL (red) time traces for a CdSe/CdS NC. (C) Histogram of the exciton relaxation times. Red, blue and green histograms correspond to relaxation times extracted from the fits to individual time traces of three different, single NCs. Black histogram shows occurrences of relaxation times extracted from averaged traces from NC clusters. (D) Histograms showing the relative contributions of the SE (blue) and the  $\Delta PL$  (red) to the total detected signal change  $S_{\text{mod}}$  and  $PL_{t^-} - PL_{t^+}$ , respectively.

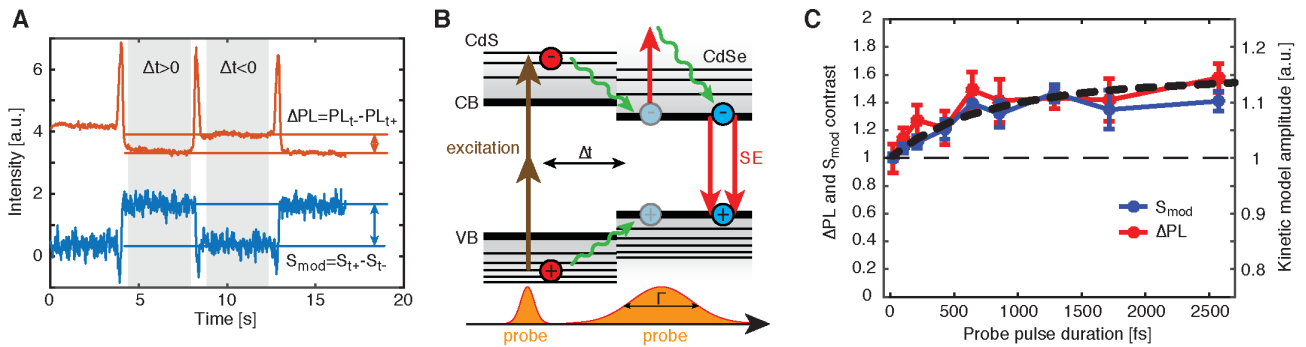


**Fig. 4. Higher stimulated emission and photo-luminescence contrast with longer probe pulse.** (A) PL and  $S_{\text{mod}}$  signals recorded in time while repeatedly scanning the interpulse delay time  $\Delta t$  from negative to positive values. (B) Concept of the varying probe pulse duration experiment. (C) Normalized  $S_{\text{mod}}$  and  $\Delta PL$  as a function of probe pulse duration. The traces were averaged from 7 (4 positively and 3 negatively chirped probe traces) separate measurements on different NC clusters. Error bars indicate the standard deviation. Black dashed line is the result of solving the set of kinetic rate equations described in Supp. Text 7.